Available online at www.sciencedirect.com
ScienceDirect
International Journal of Thermal Sciences 48 (2009) 1129–1137
International Journal of Thermal Sciences
www.elsevier.com/locate/ijts

Thermosolutal convection within a vertical porous enclosure in the case of a buoyancy ratio balancing the separation parameter

M. Er-Raki [a], M. Hasnaoui [a,*], A. Amahmid [a], M. El Ganaoui [b]

[a] *University Cadi Ayyad, Faculty of Sciences Semlalia, Physics Department, B.P. 2390, Marrakesh, Morocco*
[b] *University of Limoges, SPCTS UMR 66 38 CNRS, Faculty of Sciences and Techniques, France*

Received 27 November 2007; received in revised form 6 August 2008; accepted 22 August 2008

Available online 16 September 2008

Abstract

The present work deals with an analytical solution based on the parallel flow assumption obtained in the case of a vertical porous layer heated and salted from the long vertical sides with uniform fluxes of heat and mass, respectively. The study concerns a specific case for which the buoyancy ratio and the separation coefficient are identical. For this particular situation, the external mass flux is compensated by the Soret effect, which leads to zero concentration gradient on the vertical walls. The problem is first analyzed by solving numerically the full governing equations and the aspect ratio required to satisfy numerically the parallel flow conditions is determined. Analytical solutions for the pseudo-conductive and boundary layer regimes are proposed and discussed. The *N–Le* plane is divided into regions with specific behaviors and the results obtained are presented in terms of boundary layer thickness, heat transfer (Nusselt number), and mass transfer (Sherwood number) versus the main governing parameters.

Keywords: Soret effect; Porous medium; Thermosolutal convection; Analytical and numerical solution

1. Introduction

The study of the interaction between thermodiffusion and thermosolutal natural convection in fluid and porous media is of great importance owing to the presence of the phenomenon in several natural, environmental and industrial processes. The Soret effect could be large enough to affect considerably the flow, heat, and mass transfer characteristics in some mixtures like polymers, sodium chloride in compact clays and ferrofluids. In addition, the thermodiffusion phenomenon may engender specific behaviors in convective motions (multiplicity of solutions, super and subcritical flows, hysteresis loops, Hopf's bifurcations and reversal gradients of concentration).

Many experimental efforts have been devoted in the past to the measurement of the Soret coefficient. For binary mixtures, this coefficient is measured as the ratio of the thermo-diffusion coefficient to the molecular diffusion and the accuracy of the measurements is influenced by convection. A useful review of different techniques used to measure the Soret coefficient, was reported in a recent paper by Platten [1]. The author concluded that each method, among those existing, has its own limitation and there is no universal technique that works for measuring the Soret coefficient of any binary mixture. Bifurcations phenomena in a horizontal porous layer of normal-fluid ^{3}He–^{4}He mixture heated from below were studied experimentally by Rehberg and Ahlers [2]. Their study showed that the nature of bifurcation from the rest state depends on the separation ratio. Thermo-diffusion in a solution of sodium chloride contained in compact clay was studied experimentally by Rosanne et al. [3]. They concluded that thermal diffusion enhances the mass transfer. A comparative study of the Soret coefficient measured in a free fluid and a porous medium was conducted by Platten and Costesèque [4]. The authors reported that the coefficients measured in both media do not differ significantly.

Different aspects relative to the coupling between thermodiffusion and natural convection were investigated theoretically in previous studies. The critical conditions corresponding to the onset of convection were determined by several authors for both

* Corresponding author. Tel.: +212 24 43 46 49; fax: +212 24 43 74 10.
E-mail address: hasnaoui@ucam.ac.ma (M. Hasnaoui).

1290-0729/$ – see front matter
doi:10.1016/j.ijthermalsci.2008.08.012

Nomenclature

A	aspect ratio of the porous matrix, H'/L'
D	mass diffusivity of species
D_T	thermo-diffusion coefficient
g	gravitational acceleration
H'	height of the enclosure
j'	constant mass flux per unit area
K	permeability of the porous medium
L'	width of the porous layer
Le	Lewis number, α/D
S_P	Soret parameter, $S'_0 D_T \Delta T'/(D\Delta S')$
N	buoyancy ratio, $\beta_S \Delta S'/\beta_T \Delta T'$
Nu	Nusselt number
q'	constant heat flux per unit area
R_T	thermal Darcy-Rayleigh number, $g\beta_T K q' L'^2/(\lambda\alpha\nu)$
S	dimensionless solute concentration, $(S' - S'_0)/\Delta S'$
S'_0	reference solute concentration
Sh	Sherwood number
$\Delta S'$	characteristic solute concentration, $j'L'/D$
t	dimensionless time, $t'\alpha/(L'^2\sigma)$
T	dimensionless temperature, $(T' - T'_0)/\Delta T'$
T'_0	reference temperature
$\Delta T'$	characteristic temperature, $q'L'/\lambda$
(u, v)	dimensionless velocities in (x, y) directions, $(u'L'/\alpha, v'L'/\alpha)$
(x, y)	dimensionless coordinates, $(x'/L', y'/L')$

Greek symbols

α	thermal diffusivity
β_S	solute concentration expansion coefficient
β_T	thermal expansion coefficient
ε	normalized porosity, ε'/σ
ε'	porosity of the porous medium
λ	thermal conductivity
ν	kinematic viscosity of the fluid
$(\rho c)_f$	heat capacity of the fluid mixture
$(\rho c)_p$	heat capacity of the saturated porous medium
σ	heat capacity ratio, $(\rho c)_p/(\rho c)_f$
ψ	dimensionless stream function, ψ'/α
ζ	dimensionless vorticity, $\zeta' L'^2/\alpha$
η	relaxation factor, $(C_a K\alpha)/(\sigma L'\nu)$

Superscript

$'$	for dimensional variable

Subscripts

0	refers to a reference state
S	refers to solutal
T	refers to thermal

horizontal [5–10] and vertical [11] rectangular enclosures. The importance of such category of problems, for which the stability analysis is possible, remains in their attractive aspects characterized by the richness of the behaviors susceptible to be encountered (critical conditions of the onset of stationary and/or oscillatory convective motions and many other behaviors). Hence, Bourich et al. [5] considered the case of a horizontal porous enclosure, obeying the Brinkman–extended Darcy model and heated uniformly from below with a constant heat flux. The Soret effect on thermal natural convection was studied analytically and numerically and thresholds for the onset of stationary and finite amplitude convection are determined explicitly as function of the governing parameters. The threshold for the Hopf's bifurcation is obtained on the basis of the linear stability analysis. Thermal convection in binary liquid mixtures was considered by Ryskin et al. [6] in the limit where the solutal diffusivity is weak but the separation ratio is large. Convective motion is found to set in at Rayleigh numbers well below the critical threshold for single-component liquids. Sovran et al. [7] studied the onset of convection in an infinite porous layer saturated by a binary fluid with impermeable horizontal walls maintained at different and uniform temperatures. Using a linear stability analysis, the criteria for the onset of motion via a stationary and Hopf's bifurcation were derived for the cases of heating from below or from the top. They showed that the bifurcation from the rest state depends on, among other things, the separation ratio. Mahidjiba et al. [8] investigated analytically and numerically the interaction between the Soret effect and a shear stress applied on the free upper boundary of a horizontal fluid layer of a binary mixture. The boundaries of the system were considered impermeable to mass transfer and subjected to uniform heat fluxes. The occurrence of multiple steady-state solutions was demonstrated for given sets of the governing parameters. The onset of thermosolutal convection in a horizontal porous layer heated and salted from below and subject to a horizontal heat flux balanced by a Soret mass flux was examined by Mansour et al. [9]. They demonstrated that subcritical with or without supercritical bifurcations are possible depending on the Soret parameter. The lateral heating parameter affects the flow and the heat transfer considerably, but its effect on the mass transfer is negligible. Charrier-Mojtabi et al. [10] investigated the Soret effect under the simultaneous action of vibrational and gravitational accelerations in a porous cavity saturated by a binary mixture. The problem was examined for different aspect ratios and various directions of vibration. They found that, for both stationary and Hopf's bifurcations, the vertical vibration has a stabilizing effect while the horizontal one has a destabilizing effect on the onset of convection motion. The onset of thermogravitational diffusion in a vertical porous cavity subject to horizontal thermal gradients in the case of opposing and equal thermal and solutal buoyancy forces was examined by Marcoux et al. [11]. The thresholds of instability were computed for various enclosure aspect ratios by mean of a linear stability analysis. Their numerical results showed different flow

structures in addition to the existence of time-periodic oscillatory solutions.

Studies involving effects of both horizontal and vertical hydrodynamic and thermal heterogeneity on the onset of convection in a horizontal layer of saturated isotropic [12] and anisotropic [13] porous media, uniformly heated from below, are studied analytically using linear stability theory for the case of weak heterogeneity. Thermodiffusion combined with non-Boussinesq behaviors [14], gravity gradients [15], cross gradients of temperature and concentration [16,17], boundary layer behaviors [18] and analysis of the Soret coefficient [19] have also been the object of interest. Karcher and Müller [14] studied Bénard convection in a mixture displaying Soret effects and obeying a nonlinear density-temperature relation. Using the linear theory, they demonstrated that the non-Boussinesq properties have a destabilizing effect on the rest state regime. Combined effects of the gravity gradient and thermal diffusion on convection in a horizontal porous layer, subject to vertical gradients of temperature and concentration, were studied by Alex and Patil [15]. They found that the Soret parameter affects the pattern of convection only when its magnitude is large in the presence and in the absence of gravity gradient. Bennacer et al. [16] studied natural convection combined with Soret effect in a binary fluid saturating a shallow horizontal porous layer subjected to cross fluxes of heat and mass. They demonstrated that both natural and anti-natural flows exist in the presence of a vertical destabilizing concentration gradient. Soret effect on the multiplicity of solutions induced in a square porous cavity heated from below and subjected to a horizontal gradient of concentration was studied by Mansour et al. [17]. They observed that only one monocellular flow mode persists at large values of the buoyancy ratio both in the presence and in the absence of the Soret effect. Also, the results obtained show that some flow modes, destroyed by the solutal buoyancy forces in the absence of the Soret effect, reappear in some range of the Soret parameter. Soret effect on boundary layer flows induced in a vertical porous layer subjected to horizontal fluxes of heat and mass was studied by Er-Raki et al. [18]. It was found that different boundary layer behaviors are possible depending on the range of the Soret parameter for given values of the buoyancy ratio and the Lewis number. Jiang et al. [19] made a numerical study to investigate thermosolutal convection of a water-ethanol binary mixture, in a three-dimensional horizontal cavity, filled with an aluminium oxide (Al_2O_3). The thermal diffusion or Soret effect is analyzed globally with a separation ratio and locally with the distributions of ethanol mole fraction on the horizontal and vertical lines in the centre of the porous cavity. The effect of the pressure/(temperature) variation on the Soret coefficient of ethanol was analysed at a fixed temperature/(pressure). For both cases, the relative variation of the Soret coefficient around the mean value was found noticeable but more pronounced when the temperature was varied [$\pm 13.74\%/(\pm 26.48\%)$ as relative variation when the pressure/(temperature) was varied].

The object of the present work consists in studying analytically and numerically the interaction between thermodiffusion and imposed external fluxes of heat and mass in a vertical porous cavity. The problem of a vertical porous layer heated and salted from the long vertical sides with uniform fluxes of heat and mass was considered in the past by several authors in the absence of Soret effect (see, for instance, the references [20–22]). In addition, a configuration with prescribed heat and mass fluxes allows to tackle analytically the problem and allows a parametric study (tedious numerically) very helpful for a better understanding of the fluid flow and heat and mass transfer characteristics. In fact, the delimitation of the different regions with specific behaviors is very difficult numerically and shows how the numerical treatment of a given problem remains very insufficient particularly in the case of problems with multiple solutions. Finally, a heat flux generation or removal could be obtained in experiment while considering very poor conductive or thicker boundaries and mass flux could be generated or removed at batteries wall through endothermic or exothermic reactions [23–25]. For the present investigation, attention is mainly focused on the particular situation where the Soret parameter, defined as the ratio of the separation coefficient to the buoyancy ratio, is equal to unity. An appropriate analytical solution for the pseudo-conductive and the boundary layer regimes is derived for this particular case.

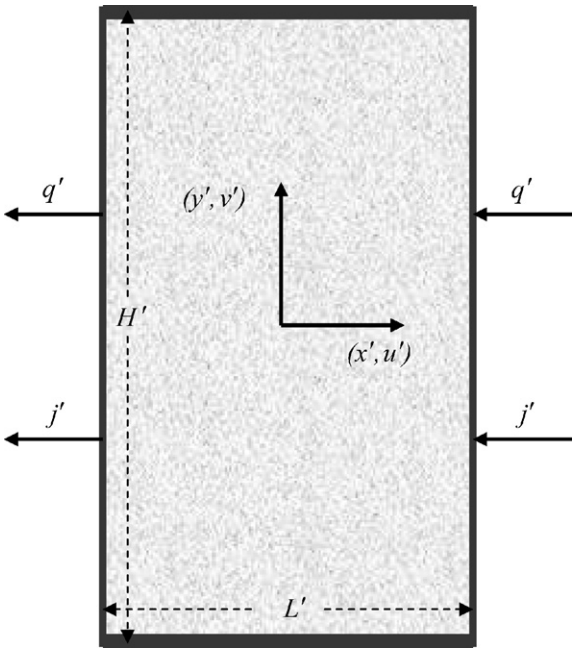

Fig. 1. Sketch of the physical system.

2. Physical problem and mathematical formulation

The geometry under consideration, sketched in Fig. 1, corresponds to an isotropic, homogeneous and saturated vertical porous layer of height H' and width L' such that $A = H'/L' \gg 1$. The vertical walls of the layer are submitted to uniform heat flux, q', and mass flux, j', while its horizontal walls are considered adiabatic and impermeable to mass transfer. Using the Darcy model and the Boussinesq approximation

and assuming constant properties, the dimensionless equations governing this problem are:

$$\eta\frac{\partial\zeta}{\partial t}+\zeta=R_T\left(\frac{\partial T}{\partial x}+N\frac{\partial S}{\partial x}\right) \tag{1}$$

$$\frac{\partial T}{\partial t}+u\frac{\partial T}{\partial x}+v\frac{\partial T}{\partial y}=\nabla^2 T \tag{2}$$

$$\varepsilon\frac{\partial S}{\partial t}+u\frac{\partial S}{\partial x}+v\frac{\partial S}{\partial y}=\frac{1}{Le}\left(\nabla^2 S+S_P\nabla^2 T\right) \tag{3}$$

$$\nabla^2\psi=-\zeta \tag{4}$$

$$u=\frac{\partial\psi}{\partial y};\qquad v=-\frac{\partial\psi}{\partial x} \tag{5}$$

The associated boundary conditions are:

$$\left.\begin{array}{lll} x=\pm 1/2,\ \psi=0, & \dfrac{\partial T}{\partial x}=1, & \dfrac{\partial S}{\partial x}=1-S_P \\ y=\pm A/2,\ \psi=0, & \dfrac{\partial T}{\partial y}=0, & \dfrac{\partial S}{\partial y}=0 \end{array}\right\} \tag{6}$$

where ζ, ψ, T, S, u and v are dimensionless vorticity, stream function, temperature, concentration and horizontal and vertical components of velocity, respectively.

In addition to the Soret parameter, S_P, three other dimensionless parameters appear in the governing equations, namely, the thermal Rayleigh number R_T, the Lewis number Le and the solutal to thermal buoyancy ratio N, respectively.

Additionally, heat and mass transfers are evaluated in terms of Nusselt, Nu, and Sherwood, Sh, numbers given, respectively, by:

$$Nu=\left(T\left(\frac{1}{2},0\right)-T\left(-\frac{1}{2},0\right)\right)^{-1}\quad\text{and}$$

$$Sh=\left(S\left(\frac{1}{2},0\right)-S\left(-\frac{1}{2},0\right)\right)^{-1} \tag{7}$$

For a better understanding of the physical phenomena occurring in this problem, an analytical method is adopted. In fact, the analytical resolution, when it is possible, allows a detailed parametric study often less evident by the numerical method especially when multiple solutions and bifurcations are possible for the considered problem. In addition, the analytical solution leads directly to mathematical correlations and allows a deeper discussion implying the main parameters controlling the fluid flow, heat and mass transfers.

3. Numerical validation of the parallel flow assumption

The main task of the present paper is the derivation of an analytical solution and its exploitation for a specific case; the numerical method is adopted here with the sole purpose of validating the analytical results. However, some numerical computations are conducted to define and qualify the geometrical domain of this study. Basic considerations of the numerical procedure are described below.

Partial Differential Equations (PDE) set (1)–(3) were discretized by using a classical central finite-difference scheme and the iterative procedure was performed by using the Alternate Direction Implicit method (A.D.I.). The stream function field was obtained from Eq. (4) using the successive over-relaxation method (S.O.R).

A global non-uniform grid was used in the x-direction by dividing the domain into three subdomains. Hence, a fine grid was used near the vertical walls ($\Delta x = 0.005$ in the boundary layer regions) while a coarse one ($\Delta x = 0.02$) was used outside the boundary layer regions. A similar procedure was also applied in the vertical direction to refine the grid in the vicinity of the horizontal walls ($\Delta y = 0.015$ near these walls against $\Delta y = 0.065$ in the remaining space). The computations were performed with a grid of 81×201 and an aspect ratio varying in the range $8 \leqslant A \leqslant 12$ (the choice of this range of A is justified in the following subsection). The mesh size considered was found enough to provide a good compromise between the required accuracy (validation of the analytical results) and the computational effort. The steady state regime is controlled by the satisfaction of the criterion $(\sum_i \sum_j |\Gamma_{i,j}^{n+1} - \Gamma_{i,j}^{n}| / \sum_i \sum_j |\Gamma_{i,j}^{n+1}|) \leqslant 10^{-5}$, where Γ stays for any of ζ, T, S and ψ.

Table 1
Parametric study for the aspect ratio effect, A, for $R_T = 500$, $Le = 10$, $N = -1.2$ and $S_P = 1$

Nature of results		ψ_0	Nu	Sh
Analytical results		3.24	5.71	89.54
Numerical results	$A = 1$	3.37	5.07	60.87
	$A = 2$	3.32	5.68	78.82
	$A = 4$	3.25	5.69	87.59
	$A = 6$	3.25	5.69	89.17
	$A = 8$	3.25	5.69	89.46
	$A = 12$	3.25	5.69	89.51

Numerous preliminary numerical tests have been conducted to identify the minimum value of the aspect ratio required to recover the analytical results with a reasonable agreement. The results obtained with the combination $(Le, N, R_T, S_P) = (10, -1.2, 500, 1)$ are summarized in Table 1. It can be seen from this table that the aspect ratio $A = 4$ is enough to validate numerically the analytical results for both ψ_0 and Nu but not for Sh. However, from $A = 8$, the numerical results recover the analytical ones with a maximum difference within 0.4%.

4. Results and discussion

4.1. The parallel flow solution

The exact analytical solution of the system of Eqs. (1)–(3) is not possible due to the strong coupling between the equations and to their non-linear character. However, in the limit of a shallow enclosure ($A \gg 1$), an approximate solution of these equations becomes possible based on the parallel flow assumption which was successfully used in the past by Cormack et al. [26] and by many other authors after that for both fluid and porous media. For the present problem, the parallel flow approximation is well confirmed numerically in terms of dynamic, thermal and solutal fields presented in Fig. 2. In fact, it is seen from this figure that, in the core region of the cavity, the flow is parallel to the long sides and the temperature and concentration

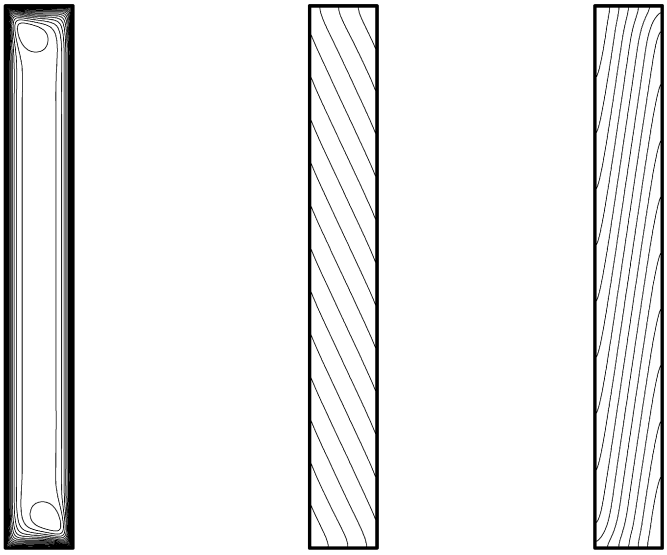

Fig. 2. Streamlines (a) isotherms (b) concentration field (c) for $R_T = 100$, $Le = 3$, $N = -3$, $S_P = 1$ and $A = 8$.

fields are characterized by a linear stratification in the vertical direction.

The PDE set describing the problem under the parallel flow assumptions and for the particular value ($S_P = 1$) is obtained as:

$$\frac{d^2\psi}{dx^2} = -R_T \frac{d}{dx}(\theta_T + N\theta_S) \tag{8}$$

$$\frac{d^2\theta_T}{dx^2} = -C_T \frac{d\psi}{dx} \tag{9}$$

$$\frac{d^2\theta_S}{dx^2} = (C_T - Le\, C_S)\frac{d\psi}{dx} \tag{10}$$

The corresponding boundary conditions on the active walls are:

$$\psi = 0, \quad \frac{d\theta_T}{dx} = 1, \quad \frac{d\theta_S}{dx} = 0 \quad \text{for } x = \pm 1/2 \tag{11}$$

By solving the resulting system (8)–(10), with the boundary conditions (11), a parallel flow solution is obtained as follows:

$$\psi(x) = k\left[1 - \frac{\cosh(\Omega x)}{\cosh(\Omega/2)}\right] \tag{12}$$

$$v(x) = k\Omega \frac{\sinh(\Omega x)}{\cosh(\Omega/2)} \tag{13}$$

$$T(x, y) = C_T y + (1 - kC_T)x + kC_T \frac{\sinh(\Omega x)}{\Omega \cosh(\Omega/2)} \tag{14}$$

$$S(x, y) = C_S y + k(C_T - Le\, C_S)x - k(C_T - Le\, C_S)\frac{\sinh(\Omega x)}{\Omega \cosh(\Omega/2)} \tag{15}$$

with

$$\Omega = \sqrt{R_T[C_T(1 - N) + N\, Le\, C_S]} \quad \text{and} \quad k = \frac{R_T}{\Omega^2} \tag{16}$$

The energy and mass balances across any horizontal section of the enclosure yield the following expressions for the parameters C_T and C_S:

$$C_T = \frac{A_1}{1 + A_0} \quad \text{and} \quad C_S = \frac{(Le\, A_0 - 1)}{(Le^2 A_0 + 1)} C_T \tag{17}$$

where

$$A_0 = k^2\left(\frac{3}{2} - \frac{3\tanh(\Omega/2)}{\Omega} - \frac{\tanh^2(\Omega/2)}{2}\right) \quad \text{and}$$

$$A_1 = k\left(1 - \frac{2\tanh(\Omega/2)}{\Omega}\right) \tag{18}$$

Then, the expressions of the Nusselt and Sherwood numbers can be deduced as:

$$Nu = \frac{1}{1 - C_T A_1} \quad \text{and} \quad Sh = \frac{1}{(C_T - Le\, C_S)A_1} \tag{19}$$

4.2. Discussion of some limiting cases

Hereafter, two limiting cases, corresponding respectively to small values (pseudo-conductive regime) and large values (boundary layer regime) of Ω will be considered. These limits lead to important simplifications of the parallel flow solution.

4.2.1. The pseudo conductive regime

Such a regime corresponds to very small values of Ω and can be observed at sufficiently small values of R_T. For this case, the parallel flow solution is reduced to the following expressions:

$$\psi(x) = \frac{R_T}{2}\left(-x^2 + \frac{1}{4}\right) \tag{20}$$

$$v(x) = R_T x \tag{21}$$

$$T(x, y) = C_T y + x + \frac{R_T C_T}{6}\left(x^3 - \frac{3}{4}x\right) \tag{22}$$

$$S(x, y) = C_S y - \frac{R_T(C_T - Le\, C_S)}{6}\left(x^3 - \frac{3}{4}x\right) \tag{23}$$

The Nusselt and Sherwood numbers corresponding to the pseudo-conductive regime are expressed as:

$$Nu = \frac{12}{12 - R_T C_T} \quad \text{and} \quad Sh = \frac{12}{R_T(C_T - Le\, C_S)} \tag{24}$$

with C_T and C_S given by:

$$C_T = \frac{10 R_T}{120 + R_T^2} \quad \text{and} \quad C_S = \frac{(Le\, R_T^2 - 120)}{(Le^2 R_T^2 + 120)} C_T \tag{25}$$

4.2.2. The boundary layer regime

The boundary layer regime can be observed when $\Omega \gg 1$ (the parameter Ω being inversely proportional to the thickness δ of the vertical boundary layer) and it corresponds to sufficiently large values R_T. In the boundary layer region, the simplified expressions of ψ, v, T and S can be given respectively under the following forms:

$$\psi(x) = k\left(1 - e^{\Omega(\lambda x - 1/2)}\right) \tag{26}$$

$$v(x) = \lambda k \Omega e^{\Omega(\lambda x - 1/2)} \tag{27}$$

$$T(x,y) = C_T y + (1 - kC_T)x + \lambda k C_T \frac{e^{\Omega(\lambda x - 1/2)}}{\Omega} \tag{28}$$

$$S(x,y) = C_S y + k(C_T - Le\,C_S)x - \lambda k(C_T - Le\,C_S)\frac{e^{\Omega(\lambda x - 1/2)}}{\Omega} \tag{29}$$

where λ is worth $1/(-1)$ for the positive/(negative) values of x.

The expressions of the parameters C_T and C_S become:

$$C_T = \frac{k\left(1 - \frac{2}{\Omega}\right)}{1 + G\left(1 - \frac{3}{\Omega}\right)} \quad \text{and}$$

$$C_S = \left(\frac{Le\,G\left(1 - \frac{3}{\Omega}\right) - 1}{Le^2 G\left(1 - \frac{3}{\Omega}\right) + 1}\right) C_T \tag{30}$$

with

$$G = k^2 \tag{31}$$

The Nusselt and Sherwood numbers expressions can be reduced to:

$$Nu = \frac{1}{1 - kC_T\left(1 - \frac{2}{\Omega}\right)} \quad \text{and}$$

$$Sh = \frac{1}{k(C_T - Le\,C_S)\left(1 - \frac{2}{\Omega}\right)} \tag{32}$$

To quantify the quantity G versus the governing parameters of the problem, an appropriate equation is established by combining Eqs. (16), (30) and (31), which yields:

$$\xi_1 G^2 - \xi_2 \Omega G - \Omega^2 = 0 \tag{33}$$

with

$$\begin{cases} \xi_1 = Le^2(\Omega - 3) \\ \xi_2 = (Le^2 + NLe + N)(\Omega - 3) + (NLe + N - 1) \end{cases} \tag{34}$$

Eq. (33) admits two solutions (G_+ and G_-) given respectively by the following expressions:

$$G_+ = \frac{\Omega}{2}\left(\frac{\xi_2 + \sqrt{\xi_2^2 + 4\xi_1}}{\xi_1}\right) \quad \text{and}$$

$$G_- = \frac{\Omega}{2}\left(\frac{\xi_2 - \sqrt{\xi_2^2 + 4\xi_1}}{\xi_1}\right) \tag{35}$$

It can be deduced from Eq. (31) that G is a positive parameter. Thus, only G_+ satisfies this condition since ξ_1 is always positive ($\Omega \gg 1$).

Furthermore, at sufficiently large values of Ω, the simplified approximate expression of the parameter G is given by:

$$G \cong \frac{Le^2 + NLe + N}{Le^2}\Omega \quad \text{for } N > \frac{-Le^2}{1 + Le} \tag{36}$$

and

$$G \cong \frac{-1}{Le^2 + NLe + N} \quad \text{for } N < \frac{-Le^2}{1 + Le} \tag{37}$$

Two boundary layer behaviors, corresponding to Eqs. (36) and (37), are to be distinguished and their corresponding solutions are termed as S_1 and S_2, respectively. Their domains of existence are determined here in terms of Le and N.

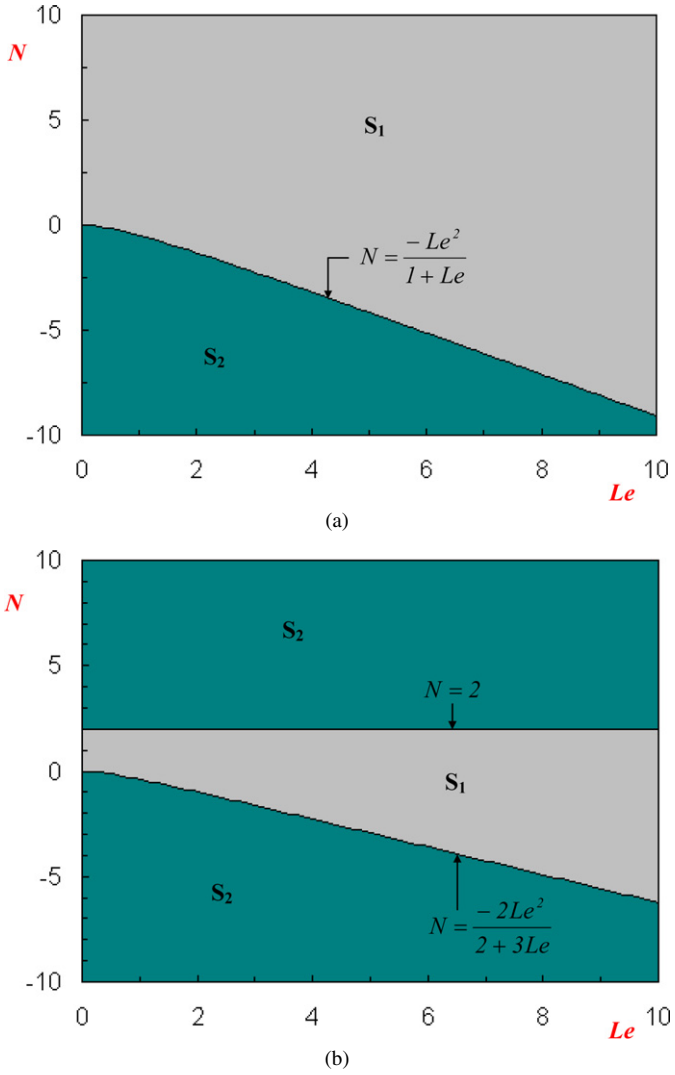

Fig. 3. Different domains in the N–Le plane corresponding to the different boundary layer behaviors for $S_P = 1$ (a) and $S_P = 1.5$ (b).

From the obtained results, it can be deduced that the boundary layer flows corresponding to aiding buoyancy forces ($N > 0$) are characterized by the existence of a unique behavior (represented by S_1) for the particular value $S_P = 1$. This result is different from that reported by Er-Raki et al. [18] and [27] who showed that, for $S_P \neq 1$, two boundary layer behaviors are possible even for positive values of N. The difference between both situations can be clearly seen by comparing Figs. 3(a) and 3(b) corresponding, respectively, to $S_P = 1$ and $S_P \neq 1$ and illustrating the different domains corresponding to the boundary layer behaviors denoted S_1 and S_2 in the N–Le plane.

Using Eqs. (36) and (37), the approximate expressions of Ω corresponding to S_1 and S_2 at sufficiently large values of R_T can be given, respectively, as follows:

$$\Omega \cong R_T^{2/5} Le^{2/5}\left(Le^2 + NLe + N\right)^{-1/5} \tag{38}$$

$$\Omega \cong R_T^{1/2}\left[-\left(Le^2 + NLe + N\right)\right]^{1/4} \tag{39}$$

From these equations, it can be easily deduced that the boundary layer thickness δ (which is inversely proportional to Ω)

increases with N. This behavior is different from that reported in [18] for $S_P \neq 1$ where it is shown that the parameter δ can increase or decrease with N depending on the sign of the latter. In addition, for $S_P \neq 1$, it was demonstrated [18] that the horizontal profiles of both temperature and concentration exhibit boundary layer behaviors (horizontal gradients nearly zero in the central part of the cavity and important gradients in a very thin layer adjacent to the vertical boundaries) for the solution S_1 but for the solution S_2, no boundary layer behavior was observed neither for the temperature nor for the concentration. Eq. (28) is also valid for $S_P \neq 1$, which means that the temperature profile keeps the same behavior independently of the value attributed to the parameter S_P. However the concentration fields exhibit different behaviors. In fact, it can be demonstrated from Eq. (29) that the concentration profiles for S_1 and S_2 present no boundary layer behavior for $S_P = 1$ while it was demonstrated in the past [18] that such a behavior is observed in the case of S_1 for $S_P \neq 1$.

5. Effects of thermal Rayleigh number and buoyancy ratio

In the following subsections, the effects of the thermal Darcy–Rayleigh number and the buoyancy ratio are examined for constant Soret parameter and Lewis number ($S_P = 1$ and $Le = 10$).

5.1. Effect of thermal Rayleigh number, R_T

Variations with R_T of Ω^{-1}, Nu and Sh are respectively presented in Figs. 4(a)–4(c) for $Le = 10$, $S_P = 1$ and $N = -3$ (for S_1) and -10 (for S_2). The analytical parallel flow solution represented in these figures by solid lines is seen to be in excellent agreement with the numerical results depicted by dotted ones. The evolution of Ω^{-1}, presented in Fig. 4(a) is characterized by a continuous decrease with R_T for both solutions. These tendencies are justified by the expressions of Eqs. (38) and (39) which show that the thickness δ (δ being proportional to Ω^{-1}) of the boundary layer, corresponding to S_1 and S_2, decreases by increasing R_T but with different slopes. In fact, from these equations, the parameter δ is seen to vary as $R_T^{-2/5}$ and $R_T^{-1/2}$ respectively for S_1 and S_2. In addition, Fig. 4(a) shows that the parallel flow and boundary layer solutions are in good agreement at sufficiently large values of R_T, which justifies the simplifications adopted in the boundary layer regime.

The evolutions of Nu and Sh with R_T, presented respectively in Figs. 4(b) and 4(c), show that these evolutions are strongly dependent on the type of behavior. In fact, for S_2, the conductive regime remains dominant in the case of Nu while the solution S_1 precipitates the appearance of the convective regime (from $R_T > 5$). For this solution, the boundary layer regime results are seen to be in good agreement with those obtained numerically and with those of the parallel flow solution; the agreement is observed from $R_T \approx 10$. The evolution of Sh, presented in Fig. 4(c), is characterized by a sharp decrease at low values of R_T, towards an asymptotic limit in the case of S_2 ($Sh_\infty \approx 11.6$) and towards a minimum ($Sh_{\min} \approx 13.04$) in the

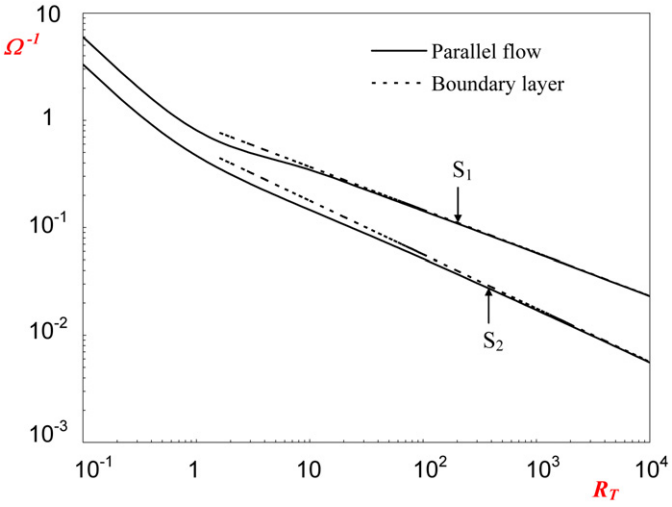

(a)

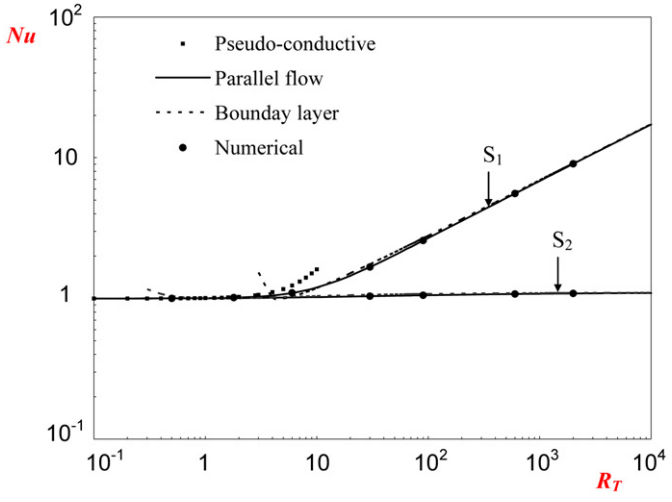

(b)

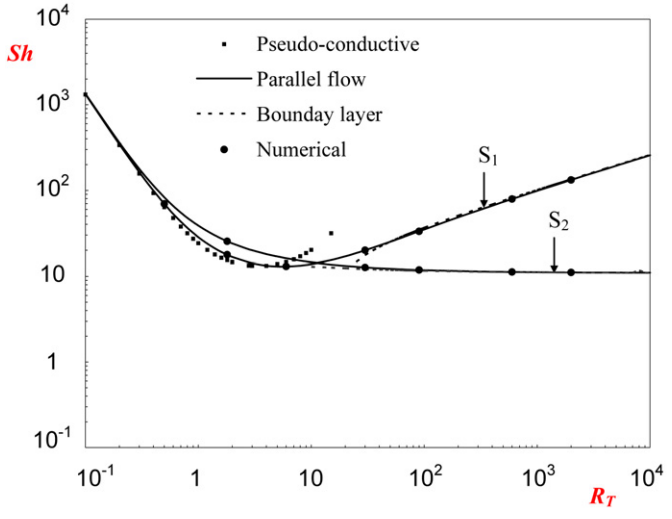

(c)

Fig. 4. Effect of R_T on Ω^{-1} (a), Nu (b) and Sh (c) for $A = 8$, $Le = 10$, $S_P = 1$, $N = -3$ (S_1) and $N = -10$ (S_2).

case of S_1, reached at $R_T \approx 6$. Beyond the minimum, *Sh* corresponding to S_1 increases linearly with R_T. It is to note that, both solutions S_1 and S_2 lead to the same results in the pseudo conductive regime (regime observed at low values of R_T) and the difference begins with the appearance of the convective motion. The validity of the analytical expressions deduced for the pseudo-conductive and the boundary layer regimes is proved in Figs. 4(b) and 4(c). In fact, a good agreement between the results based on the parallel flow solution corresponding to Eq. (19) and those of the pseudo conductive and boundary layer regimes is observed at sufficiently small and large values of R_T, respectively. Finally, it is to outline that, in pure diffusive regime, *Nu* and *Sh* are governed by Eq. (24) and their respective values in this regime (obtained by tending R_T towards 0) are 1 and infinity (equality of concentrations on the vertical walls of the cavity).

5.2. *Effect of the buoyancy ratio, N*

The effect of solutal to thermal buoyancy ratio, N, on Ω^{-1}, *Nu* and *Sh* is illustrated in Figs. 5(a)–5(c) for $R_T = 100$, $S_P = 1$ and $Le = 10$ (with $|N| = N$ in the case of S_1 ($N > 0$) and $|N| = -N$ in the case of S_2 ($N < 0$)). The effect of $|N|$ on these quantities is seen to depend strongly on the type of solution. In the case of S_1, Fig. 5(a) shows that the evolution of Ω^{-1} with $|N|$ is monotonous, characterized by a very slow increase in the range of relatively small $|N|$ and a very fast increase when this parameter exceeds 500 leading to important values of the boundary layer thickness. This means that the boundary layer behavior is observed only for relatively low values of $|N|$ in the case of S_1. The situation is different in the case of S_2 since the evolution of Ω^{-1} with $|N|$ for this case is characterized by a monotonous decrease. Hence, for S_2, the boundary layer behavior is observed for relatively large values of $|N|$. These results are well confirmed in Figs. 5(b) and 5(c) where the agreement between the parallel flow and boundary layer results is observed at sufficiently small values of $|N|$ (heat-transfer-driven flow) and sufficiently large values of $|N|$ (mass-transfer-driven flow), respectively for S_1 and S_2. In the other hand, the variations of *Nu* and *Sh* versus $|N|$ are characterized, in the case of S_1, by an increase towards asymptotic limits (not yet reached in the curve). It is of interest to note that, since Ω is small enough at sufficiently large values of N, these limits coincide with those of the expressions given by Eq. (24); they are about 5.66 and 920.11, respectively, for *Nu* and *Sh*. Physically, though the value of Ω is small, the solution is not that of a pseudo conductive regime since *Nu* is different from unity and the value of R_T is relatively important. For the solution S_2, the corresponding curves show that *Sh* increases by increasing $|N|$ while *Nu* decreases towards unity (i.e. the value of the pure diffusive regime).

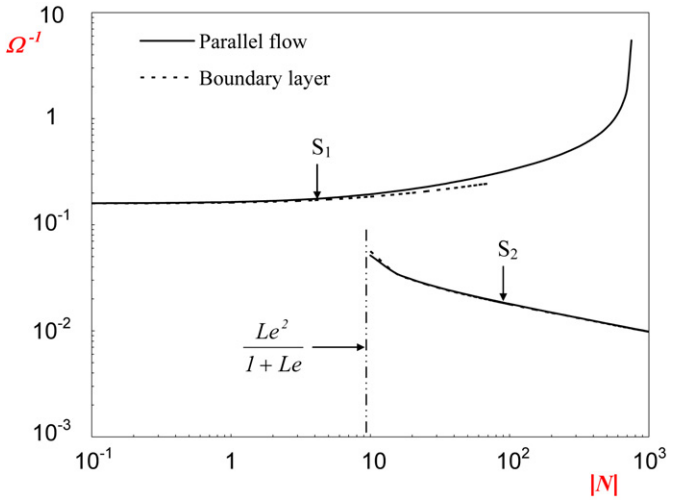

(a)

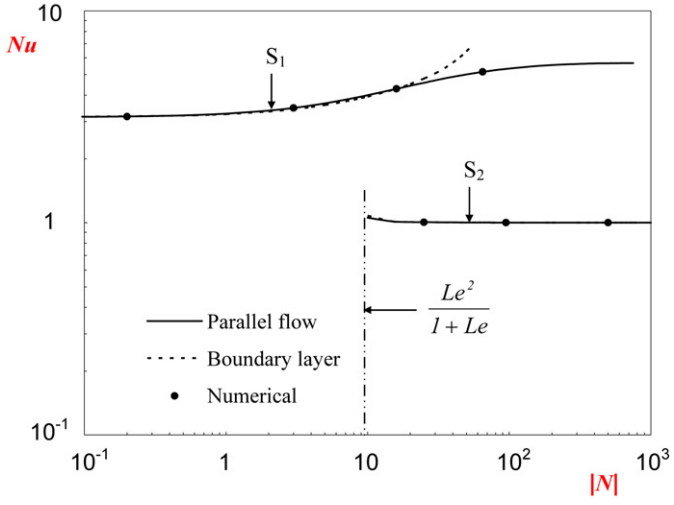

(b)

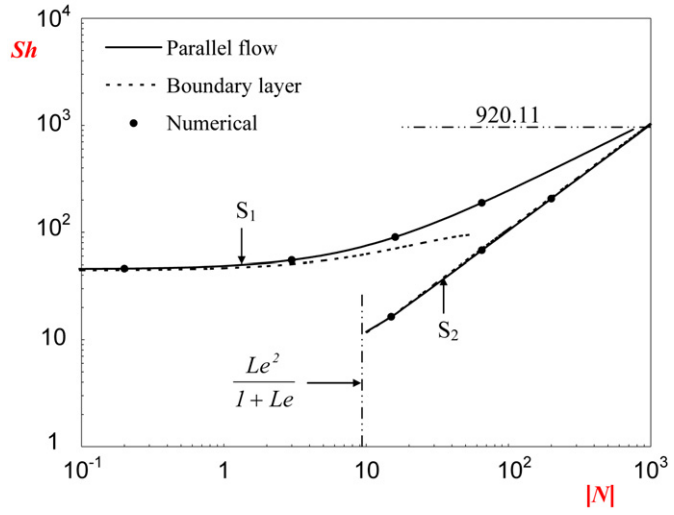

(c)

Fig. 5. Variations with $|N|$ of Ω^{-1} (a), *Nu* (b) and *Sh* (c) for $R_T = 100$, $Le = 10$, $S_P = 1$ and $A = 8$.

6. Conclusion

Soret effect on fluid flow and heat and mass transfers induced by double-diffusive natural convection in a vertical

porous enclosure subject to horizontal gradients of temperature and concentration is studied analytically and numerically. The study is conducted in the case where the external mass flux is compensated by the Soret effect ($S_P = 1$). It is found that, dependently on the region considered in the *Le*–*N* plane, two different behaviors are possible and the disappearance of the boundary layer regime may occur at sufficiently large or sufficiently small values of $|N|$. It is also found that the boundary layer comportment is absent in the concentration profile for both regions while in the case of temperature, the boundary layer behavior is possible depending on the region considered in the *Le*–*N* plane.

References

[1] J.K. Platten, The Soret effect: a review of recent experimental results, Journal of Applied Mechanics 73 (2006) 5–15.

[2] I. Rehberg, G. Ahlers, Experimental observation of a codimension-two bifurcation in a binary fluid mixture, Physical Review Letters 55 (1985) 500–503.

[3] R. Rosanne, M. Paszkuta, E. Tevissen, P.M. Adler, Thermodiffusion in a compact clay, Journal of Colloid and Interface Science 267 (2003) 194–203.

[4] J.K. Platten, P. Costesèque, The Soret coefficient in porous media, Journal of Porous Media 7 (4) (2004) 317–329.

[5] M. Bourich, M. Hasnaoui, A. Amahmid, M. Mamou, Onset of convection and finite amplitude flow due to Soret effect within a horizontal sparsely packed porous enclosure heated from below, Int. J. Heat and Fluid Flow 26 (2005) 513–525.

[6] A. Ryskin, H.W. Müller, H. Pleiner, Thermal convection in binary fluid mixtures with a weak concentration diffusivity, but strong solutal buoyancy forces, Physical Review E 67 (2003) 1–8.

[7] O. Sovran, M.C. Charrier-Mojtabi, A. Mojtabi, Naissance de la convection thermo-solutale en couche poreuse infinie avec effet Soret, C. R. Acad. Sci. Paris 329 (2001) 287–293.

[8] A. Mahidjiba, R. Bennacer, P. Vasseur, Flows in a fluid layer induced by the combined action of a shear stress and the Soret effect, Int. J. Heat Mass Transfer 49 (2005) 1403–1411.

[9] A. Mansour, A. Amahmid, M. Hasnaoui, M. Mamou, Onset of thermosolutal convection in a shallow porous layer heated and salted from below and subject to a horizontal heat flux balanced by a Soret mass flux, Int. J. Heat Mass Transfer 50 (2007) 2148–2160.

[10] M.C. Charrier-Mojtabi, Y.P. Razi, K. Maliwan, A. Mojtabi, Influence of vibration on Soret-driven convection in porous media, Numerical Heat Transfer, Part A 46 (2004) 981–993.

[11] M. Marcoux, M.C. Charrier-Mojtabi, A. Bergeon, Naissance de la thermogravitation dans un mélange binaire imprégnant un milieu poreux, Entropie 214 (1998) 31–36.

[12] D.A. Nield, A.V. Kuznetsov, The effect of combined vertical and horizontal heterogeneity on the onset of convection in a bidisperse porous medium, Int. J. Heat Mass Transfer 50 (2007) 3329–3339.

[13] D.A. Nield, A.V. Kuznetsov, The effects of combined horizontal and vertical heterogeneity and anisotropy on the onset of convection in a porous medium, Int. J. Thermal Sciences 46 (2007) 1211–1218.

[14] C. Karcher, U. Mûller, Bénard convection in binary mixture with a nonlinear density–temperature relation, Phys. Rev. E 49 (1994) 4031–4043.

[15] S.M. Alex, P.R. Patil, Effect of variable gravity field on Soret driven thermosolutal convection in a porous medium, Int. Commun. Heat Mass Transfer 28 (2001) 509–518.

[16] R. Bennacer, A. Mahidjiba, P. Vasseur, H. Beji, R. Duval, The Soret effect on convection in a horizontal porous domain under cross temperature and concentration gradients, Int. J. Numer. Meth. Heat Fluid Flow 13 (2003) 199–215.

[17] A. Mansour, A. Amahmid, M. Hasnaoui, M. Bourich, Multiplicity of solutions induced by thermosolutal convection in a square porous cavity heated from below and submitted to horizontal concentration gradient in the presence of Soret effect, Numerical Heat Transfer, Part A 49 (2006) 69–94.

[18] M. Er-Raki, M. Hasnaoui, A. Amahmid, M. Mamou, M. Bourich, Soret effect on double-diffusive boundary layer flows in a vertical porous cavity, Journal of Porous Media 10 (8) (2007) 783–795.

[19] C.G. Jiang, T.J. Jaber, H. Bataller, M.Z. Saghir, Simulation of Ludwig–Soret effect of a water–ethanol mixture in a cavity filled with aluminium oxide powder under high pressure, Int. J. Thermal Sciences 47 (2008) 126–135.

[20] O.V. Trevisan, A. Bejan, Mass and heat transfer by natural convection in a vertical slot filled with porous medium, Int. J. Heat Mass Transfer 29 (1986) 403–415.

[21] F. Alavyoon, On natural convection in vertical porous enclosures due to prescribed fluxes of heat and mass at the vertical boundaries, Int. J. Heat Mass Transfer 36 (1993) 2479–2498.

[22] M. Mamou, P. Vasseur, E. Bilgen, Double-diffusive convection instability problem in a vertical porous enclosure, J. Fluid Mech. 368 (1998) 263–289.

[23] F. Alavyoon, A. Eklund, F.H. Bark, R.I. Karlsson, D. Simonsson, Theoretical and experimental studies of free convection and stratification of electrolyte in a lead-acid cell during recharge, Electrochimica Acta 36 (14) (1991) 2153–2164.

[24] F. Alavyoon, Unsteady natural convection and mass transfer in copper electrolysis with a supporting electrolyte, Electrochimica Acta 37 (2) (1992) 333–344.

[25] A. Eklund, F. Alavyoon, R.I. Karlsson, Theoretical and experimental studies of free convection and stratification of electrolyte in a copper refining cell – II. Influence of the supporting electrolyte, Electrochimica Acta 37 (4) (1992) 695–704.

[26] D.E. Cormack, L.G. Leal, J. Imberger, Natural convection in a shallow cavity with differentially heated end walls, Part 1: Asymptotic theory, J. Fluid Mechanics 65 (1974) 209–230.

[27] M. Er-Raki, M. Hasnaoui, A. Amahmid, M. Mamou, Soret effect on the boundary layer flow regime in a vertical porous enclosure subject to horizontal heat and mass fluxes, Int. J. Heat Mass Trasfer 49 (2006) 3111–3120.